

Supplementary materials

Supplementary Equation 1

US_rad_score=

$$-6.3118 - 0.9966 \times F1 + 0.1545 \times F2 + 2.1352 \times F3 + 0.0089 \times F4 + 2.5288 \times F5$$

where the selected radiomic features ($F1$ to $F5$) are defined as follows:

- $F1$: Maximum Probability from GLCM (LoG filter, $\sigma = 2.0$ mm, 3D)
- $F2$: Autocorrelation from GLCM (original image)
- $F3$: Elongation (2D shape)
- $F4$: Minor Axis Length (2D shape)
- $F5$: Dependence Entropy from GLDM (LoG filter, $\sigma = 3.0$ mm, 3D)

Note: GLCM = Gray Level Co-occurrence Matrix; GLDM = Gray Level Dependence Matrix.

Filter parameters (σ values) are in mm.

Supplementary Equation 2

MRI_rad_score = $-0.1630 + 0.0002 \times F1 - 0.0001 \times F2 - 0.3282 \times F3$

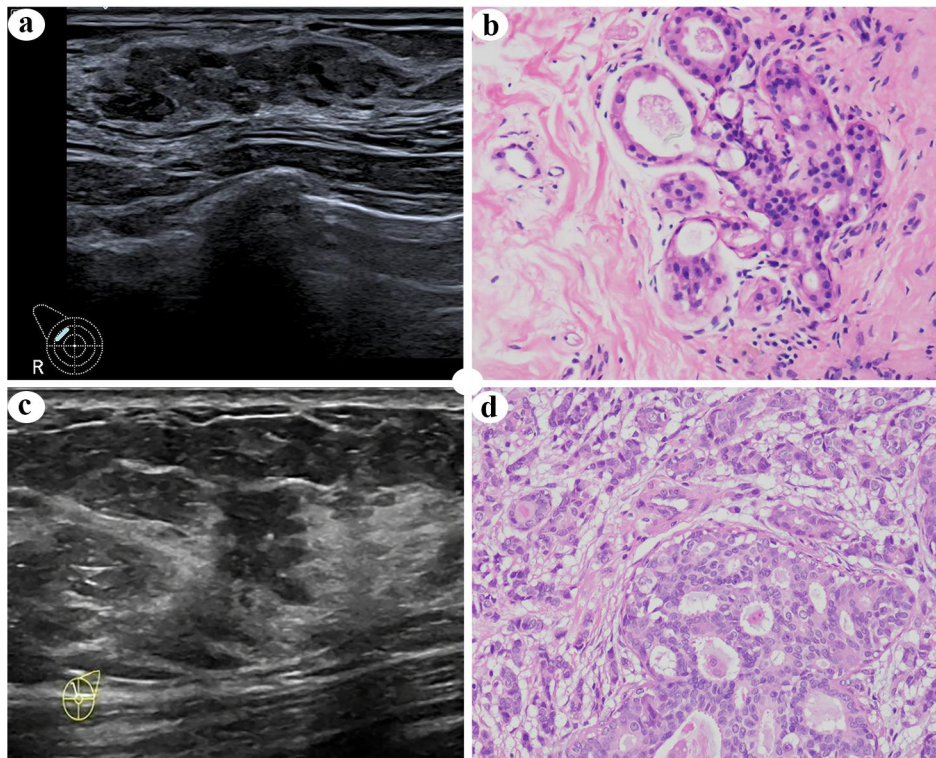
where the selected radiomic features ($F1$ to $F3$) are defined as follows:

- $F1$: Energy from first-order statistics (LoG filter, $\sigma = 2$ mm, 3D)
- $F2$: Coarseness from NGTDM (original image)
- $F3$: Gray-Level Non-Uniformity Normalized from GLSZM (original image)

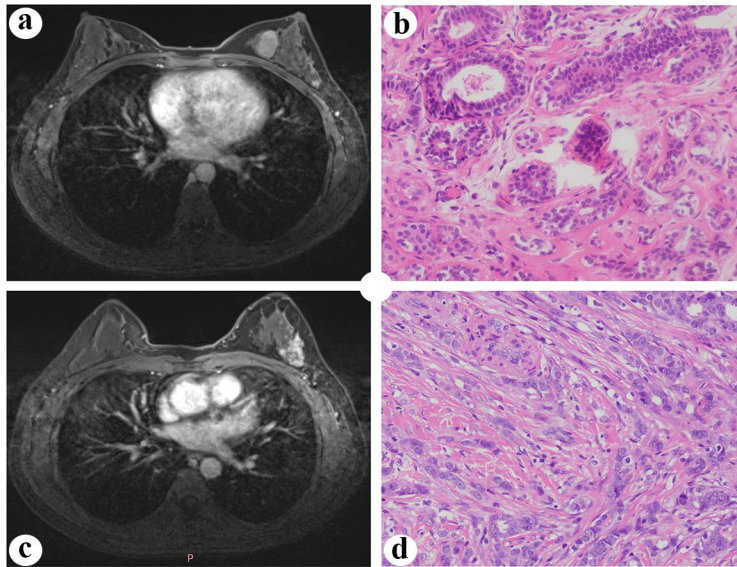
Note: NGTDM = Neighbouring Gray Tone Difference Matrix; GLSZM = Gray-level Size Zone

Matrix. Filter parameters (σ values) are in mm.

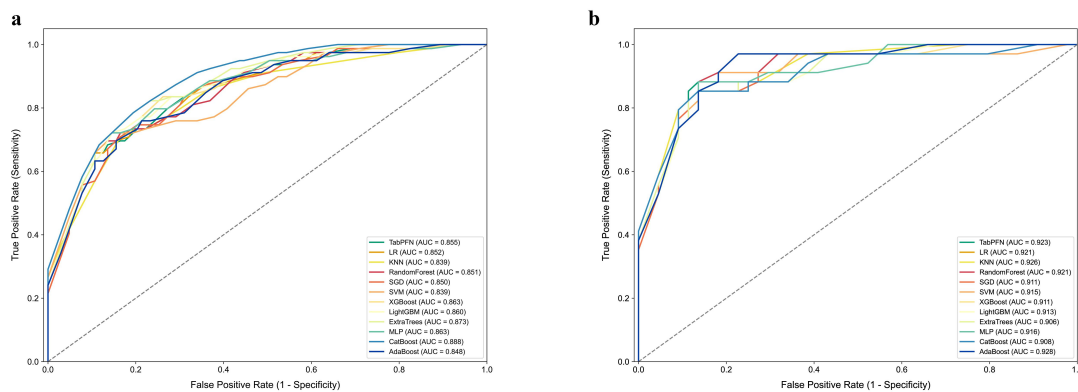
Supplementary figures and figure captions



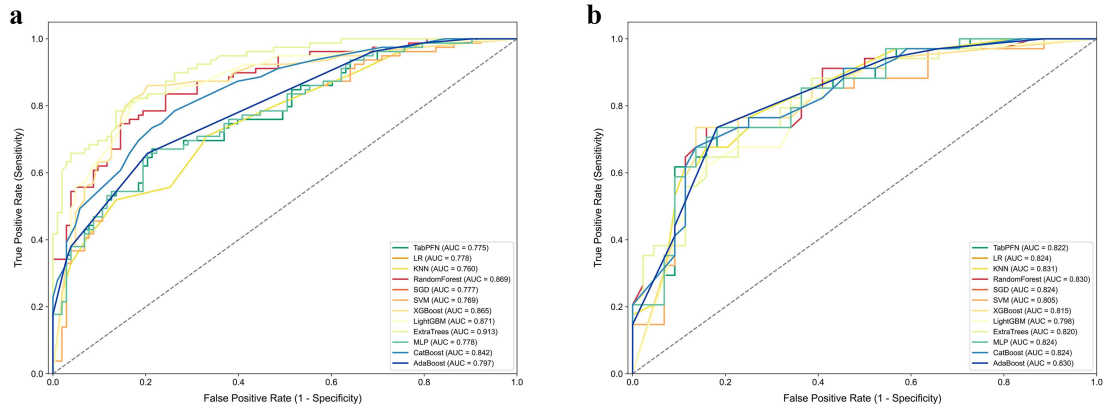
Supplementary Figure S1 Representative ultrasound BI-RADS features of adenosis and carcinoma. (a, b) Ultrasound image of a 38-year-old woman shows an oval mass with a circumscribed margin and scarce vascularity (body mark in the lower left corner). The lesion was surgically resected and confirmed to be adenosis. (c, d) Ultrasound image of a 47-year-old woman shows an irregular mass with an ill-defined margin, un-parallel orientation, microcalcifications, and internal vascularity (body mark in the lower left corner). The mass was surgically removed and diagnosed as invasive carcinoma. BI-RADS, Breast Imaging Reporting and Data System.



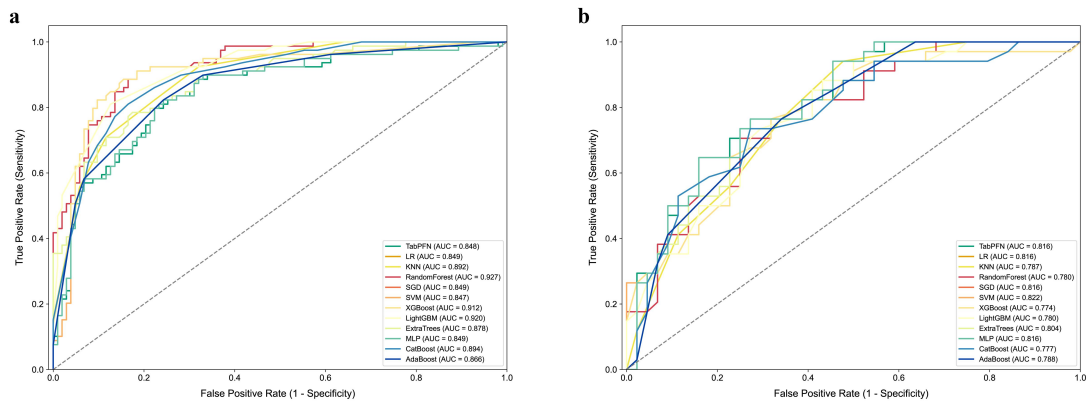
Supplementary Figure S2 Representative MRI BI-RADS features of adenosis and carcinoma. (a, b) Contrast-enhanced MR image of a 23-year-old woman shows a round mass with mild homogeneous enhancement and circumscribed margins. The lesion was assessed as BI-RADS 4a on MRI but was pathologically diagnosed as fibroadenosis. (c, d) Axial contrast-enhanced MR image of a 46-year-old woman shows an irregular mass with heterogeneous enhancement and spiculated margins. The mass was surgically confirmed to be invasive carcinoma.



Supplementary Figure S3 Comparison of classifier algorithms for the BI-RADS model. Area under the the receiver operating characteristic curve (AUC) values for the model implemented with different classifiers are presented for the (a) training and (b) testing cohorts.



Supplementary Figure S4 Comparison of classifier algorithms for the US_Rad model. Area under the the receiver operating characteristic curve (AUC) values for the model implemented with different classifiers are presented for the (a) training and (b) testing cohorts.



Supplementary Figure S5 Comparison of classifier algorithms for the MRI_Rad model. Area under the the receiver operating characteristic curve (AUC) values for the model implemented with different classifiers are presented for the (a) training and (b) testing cohorts.

Supplementary table

Table 1. Definition of features used in radiomics signatures

Variable	Full Feature Name	Feature Class	Image Type	Filter (σ)	Dimension
	Maximum Probability	GLCM	LoG-filtered	2.0 mm	3D
	Autocorrelation	GLCM	Original	—	2D/3D
	Elongation	Shape (2D)	Original	—	2D
	Minor Axis Length	Shape (2D)	Original	—	2D
	Dependence Entropy	GLDM	LoG-filtered	3.0 mm	3D
	Energy	First-order	LoG-filtered	2.0 mm	3D
	Coarseness	NGTDM	Original	—	3D
	Gray-Level Non-Uniformity Normalized	GLSZM	Original	—	3D